Available online at www.sciencedirect.com
ScienceDirect
European Journal of Pharmaceutics and Biopharmaceutics 70 (2008) 402–408
European Journal of Pharmaceutics and Biopharmaceutics
www.elsevier.com/locate/ejpb

Research paper

The consequences of granulate heterogeneity towards breakage and attrition upon fluid-bed drying

Florentine Nieuwmeyer [a,*], Kees van der Voort Maarschalk [a,b], Herman Vromans [a,c]

[a] Department of Pharmaceutics, Organon part of the Schering Plough Corporation, Oss, The Netherlands
[b] Department of Pharmaceutical Technology and Biopharmacy, Groningen University Institute for Drug Exploration (GUIDE), Groningen University, Groningen, The Netherlands
[c] Department of Pharmaceutics, Utrecht Institute for Pharmaceutical Sciences (UIPS), Utrecht University, Utrecht, The Netherlands

Received 19 November 2007; accepted in revised form 5 March 2008
Available online 18 March 2008

Abstract

High-shear granulated lactose granulates were dried in a fluid-bed dryer at various conditions. Granules were characterized by water content and size analysis. It is shown that the drying process is very dynamic in terms of growth and breakage phenomena. Granular size heterogeneity, composition and water content determine the granule behavior upon drying. Large granules consist of small primary particles and contain more water than small granules that consist of large primary particles. This differentiates the drying rate and extent of size reduction of the different granule size classes. The results enable a critical evaluation of process control and process monitoring. Understanding of granule behavior and continuous monitoring of the fluid-bed drying process enables process and product optimization.

Keywords: Breakage; Composition; Fluid-bed drying; Granule; Heterogeneity; High- shear; Lactose; Water

1. Introduction

Granulation is a common unit operation in the manufacturing of oral dosage forms. Granules are often prepared by wet processes which have been studied extensively (e.g., [1–6]). Remarkably, the subsequent drying step has received relatively little attention. In batch production, drying is often the bottleneck either for time or product quality reasons. In the fluid-bed drying process attrition, an unwanted size reduction phenomenon which leads to the formation of fines is considered a product quality diminishing side effect [7,8]. The deteriorating effects of attrition on flowability of powder masses [7] or on homogeneity of granulate [9] have been described. To prevent unwanted attrition or breakage during the fluid-bed drying process, better process understanding is needed.

In our previous study [10] it has been shown that the extent of attrition and breakage during drying is primarily dependent on the amount of water present in the granules. In fact three different domains can be distinguished. Initially at a water level above 9% the net result of applied stress becomes positive, i.e., granule growth is observed. At intermediate water content (2–9%) a plateau exists where a change in water content does not really alter the resistance to breakage. Finally, at low moisture levels con-

Abbreviations: γ, surface tension [Nm]; $d_{3,2}$, surface mean diameter [μm]; $\Delta d_{10,\mathrm{norm}}$, change in cumulative 10% frequency undersize [μm]; $\Delta d_{50,\mathrm{norm}}$, change in cumulative 50% frequency undersize (median granule size) [μm]; $\Delta d_{90,\mathrm{norm}}$, change in cumulative 90% frequency undersize [μm]; ε, porosity [-]; H, mass ratio of liquid to solid [-]; KF, Karl Fischer; μ, viscosity [Pa s]; NIR(S), near infrared (spectroscopy); PAT, process analytical technology; PC, principal component; PCA, principal component analysis; PLS(R), partial least squares (regression); ρ_s, density of the particle relative to the density of the (binder) liquid [-]; σ_c, static granule strength [Pa]; σ_v, dynamic granule strength [Pa]; S, saturation level [-]; SEC, standard error of calibration; SECV, standard error of cross validation; SEP, standard error of prediction; SNV, standard normal variance; T_{in}, inlet air temperature [°C]; v_p, relative velocity of the moving particles [m s^{-1}].

* Corresponding author. Department of Pharmaceutics, Organon part of the Schering Plough Corporation, P.O. Box 20, Molenstraat 110 Room RP2130, 5340 BH Oss, The Netherlands. Tel.: +31 412662342; fax: +31 412662524.
E-mail address: fjsnieuwmeyer@yahoo.com (F. Nieuwmeyer).

0939-6411/$ - see front matter © 2008 Elsevier B.V. All rights reserved.
doi:10.1016/j.ejpb.2008.03.003

siderable attrition and breakage is apparent. These outcomes have been explained on the basis of strength or resistance to breakage of the granules. Granule strength has been related to water content by Rumpf [1] and Schubert [11]. Rumpf [1] described granule strength in terms of saturation level (S), porosity (ε) and starting material characteristics as $d_{3,2}$ and γ. This is expressed as

$$\sigma_c = 6S\frac{(1-\varepsilon)}{\varepsilon}\frac{\gamma}{d_{3,2}} \quad (1)$$

where σ_c is static granule strength, γ is surface tension of the binder solution and $d_{3,2}$ is the surface mean diameter of the primary particles. The static granule strength describes the forces acting between two particles related to a capillary liquid bridge. When applying this equation it is assumed that the rate of granule deformation upon impact is low. When the primary particle size, porosity, surface tension of the binding agent and granule porosity are considered to be constant, the saturation level is hence the most important variable in this equation. The saturation level of a granule is defined as the ratio of pore volume occupied by liquid to the total volume of pores available in the granule. This can be expressed as

$$S = \frac{H(1-\varepsilon)}{\varepsilon}\rho_s \quad (2)$$

where H is the mass ratio of liquid to solid, ε is the intragranular porosity and ρ_s is the density of the particles relative to the density of the liquid [12].

In contrast to the theory of the static strength Ennis et al. [13] showed that at relatively low particle velocities the viscous force determines the strength of a liquid bridge. Therefore, during the dynamic fluid-bed drying process, the so-called dynamic granule strength describes the granular strength more accurately. The tensile strength of a granule under dynamic conditions is derived by the following equation:

$$\sigma_v = \frac{9}{8}\frac{(1-\varepsilon)^2}{\varepsilon^2}\frac{9\pi\mu v_p}{16 d_{3,2}} \quad (3)$$

in which μ is the viscosity and v_p is the relative velocity of the moving particles. This equation is based on the general equation for tensile strength of a granule as developed by Rumpf [1], the Reynolds equation describing the viscous force of liquid bridge and the Kozeny model [2]. In contrast to Eq. (1) where the static strength of the granules is highly dependent on the saturation level of the granules, it is assumed that the dynamic strength of the granules is dependent on the number of contact points between the moving particles in combination with the viscous force at the contact point and insensitive to the liquid saturation within certain limits [2].

It has been demonstrated that, due to preferential growth [14] of particles granulated with low viscosity binder in high-shear granulation, larger granules consist of small primary particles whereas smaller granules contain larger primary particles [2,15]. By the difference in internal composition the small granules contain relatively less water than bigger ones [16]. As a consequence, Eqs. (1)–(3) show that large granules are stronger than small granules. In high-shear granulation this heterogeneity leads to a granule size dependent difference in behavior throughout the process [2,17]. Therefore, it is important not only to study the bulk behavior during the drying process but also the effects in the different size classes.

Current FDA Process Analytical Technology (PAT) guidance stresses the importance of process understanding and control. The guidance is intended to support innovation and efficiency in pharmaceutical development, manufacturing and quality assurance. Process Analytical Technology is a system for designing, analyzing, and controlling manufacturing through timely measurements (i.e., during processing) of critical quality and performance attributes of raw and in-process materials and processes with the goal of ensuring final product quality [18]. Product quality assurance can only be achieved by knowledge of the critical process steps. Starting point of the quality by design approach is a thorough understanding of the potential risks, which is based on an in-depth knowledge of the processes involved. A robust process results when all critical parameters are "in control". Therefore, the critical parameters should be monitored constantly. Currently the fluid-bed drying process is most often controlled by monitoring the temperature and humidity of the incoming and outgoing air. Usually the process is considered to be finished when the humidity of the outgoing and incoming air is equal. The monitoring of these values does not enable absolute water content measurements in the granular bed. In the fluid-bed drying process three drying phases can be distinguished based upon the evaporation velocity of water; the constant rate period when granular surface water is abundantly present, the falling rate period when evaporation velocity decreases due to the limited presence of water at the granular surface finally ending in the equilibrium period. The possibilities of near infrared (NIR) inline measurement of water content or other granular characteristics in fluid-bed granulation or fluid-bed drying has been acknowledged (e.g., [19–23]). By NIR it is possible to measure the water content of the granules directly which enables both determination of the process stage and the end-point determination [16].

The objective of this study was to determine critical factors influencing the granule behavior during the fluid-bed drying process and to understand the process related growth and breakage phenomena.

2. Materials and methods

2.1. Fluid-bed drying

Twelve kilograms of lactose 200 M (DMV-Fonterra, Veghel, The Netherlands) was granulated in a high-shear mixer (Gral 75, Colette, Wommelgem, Belgium) for 5 min

(mixer rotation rate 150 rpm, chopper rate 1500 rpm). 1585 ml de-mineralized water was used as binding liquid. The water was poured onto the moving powder bed. The wet granules were divided in 1 kg portions and transferred to a fluid-bed dryer (Granulator Niro Aeromatic MP-1, Bubendorf, Switzerland). The equipment was heated for 30 min before use with the following parameters: inlet temperature 60 °C, air flow 60 $m^3 h^{-1}$ (1.8 $m s^{-1}$), product temperature 20 °C. Product temperature was set at 20 °C throughout the drying process. By an automated system, intrinsic to the equipment, the system is regulated by the temperature of the incoming air. In the fluid-bed drying experiments inlet air temperature (40 and 60 °C) and inlet air flow 60, 70, 80 or 100 $m^3 h^{-1}$ were varied. 60, 80 or 100 $m^3 h^{-1}$ correspond with linear velocities of 1.8, 2.4, 3.0 $m s^{-1}$ based on the type of air distribution grid. All various combinations of parameters were tested in order to evaluate the influence of process settings on particle breakage. For each combination of parameters except 70 $m^3 h^{-1}$ (inlet air temperature and air flow) the drying time was varied between 2, 3, 4, 5, 6, 8, 10, 12 and 15 min.

2.2. Granule characterization

Starting at $t = 0$, every minute a sample for reference water content determination was collected. The water content of the granules was determined with an automated Karl Fischer titration (KF coulometer 756 K with oven sample processor 774 at 150 °C, Metrohm, Herisau, Switzerland). For each sampled granular fraction the water content was determined in twofold. Furthermore, determination of the water content in granules at $t = 0$ and $t = 15$ is assumed to be most difficult. To verify these data the water content of these granules is determined for 32 experiments. Since it is assumed that if the SD for all these experiments does not exceed 0.3% the method can be assumed valid for the whole experimental set. The coulometer has been calibrated before every analysis (maximum of 28 samples) with sodium ditartrate (mean water content 15.5%, SD 0.3%). Particle size distribution of the wet and dried granules was determined by sieving 100 g of granule samples on a Retsch AS 200 control sieve (Haan, Germany). The mean particle size of the samples was estimated as a median weight-based diameter. The effect of the sieving equipment on the attrition and breakage of granules was assessed. It was found that sieving of the granules did not significantly influence the obtained results from the granulator experiments. All sieving test were performed at least in threefold.

2.3. Near infrared (NIR) water content analysis during fluid-bed drying

For the optimization of the drying regime and continuous monitoring of the water content an in-line NIR system was used as described in [16]. Before measurement the NIR was automatically calibrated by a 100% reflection standardization measurement. The NIR probe (FOSS NIRSystem Analyzer, software package Vision®, Birchwood, UK) was placed into the wall of the fluid-bed dryer at the same height of the system integrated sampling probe. Probe position was optimized by spectral analysis to ensure continuous, reliable and accurate monitoring. The NIR probe was secured tightly in the wall of the vessel to obtain stable recordings and to prevent influence of the probe on the process or the product. In-line diffuse reflectance NIR spectra were recorded every 30 s, starting at the same time point as the drying process. Each spectrum is the average of 32 individual scans in the wavelength region between 1100 and 1900 nm, with a resolution of 2 nm. NIR data analysis was done using the software package Vision® (Birchwood, UK). A quantitative water content model for lactose was created based on the first O–H overtone (1350–1500 nm). First derivative spectra (Savitsky–Golay) were normalized (SNV) prior to PLS regression analysis.

Calibration of the PLS model was quantified by standard error of calibration (SEC), indicating the fit between NIR spectra with off-line derived water content values. Validation and optimization of the number of PLS factors were done by full cross-validation. During validation, the standard error of cross-validation (SECV) was calculated. It is expected that the SECV represents the SEP (standard error of prediction). The SEP is used to evaluate the uncertainty of the future predictions [16]. Sample selection and identification was based upon mahalanobis distance determinations [24]. From this function the probability that the given sample belongs to the distribution represented by the model based spectral set can be calculated. Qualification of the spectra for quantitative use was based upon maximum distance in wavelength space.

3. Results and discussion

During the fluid-bed drying process the granules collide with each other as well as with the wall of the drying vessel. As a result granule attrition and fines formation takes place.

In Fig. 1 the granule size for the largest (d_{90}), median (d_{50}) and smallest granules (d_{10}) is shown throughout the fluid-bed drying process. In addition the formation of fines is shown. In this paper the definition of fines is arbitrarily set at particles <100 μm. Whereas the largest granules show a size increase in the first minutes of drying the smaller granules show a size decrease throughout the entire drying process. The initial growth of the larger granules is annihilated upon further drying. As can be seen, the granules undergo significant size changes during the process, suggesting a highly dynamic situation. Apparently not only during the granulation process itself [2,4,5,9], but also during the subsequent drying step constant growth and breakage phenomena occur. It has been demonstrated that within a batch of granules, prepared by high-shear granulation, differences in granule composition exist [2,10]. More specifically, the large granules contain smaller primary par-

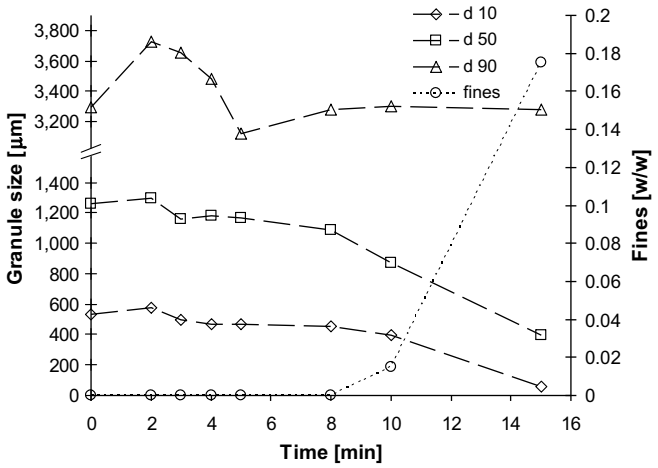

Fig. 1. Granule size (d_{10}, d_{50}, d_{90}) versus drying time throughout the fluid-bed drying process. Temperature incoming air (T_{in}) 40 °C, air velocity 1.8 m s^{-1}. On the right-hand axis the formation of fines is shown. At the start of the drying process the average d_{10} is 512 μm (standard deviation 40 μm), the d_{50} is 1285 μm (standard deviation 63 μm) and the value for the d_{90} is 3289 μm (standard deviation 212 μm). After 15 min of drying, based upon NIR read-outs, the granules were considered to be completely dried (water content <0.1%) [16].

ticles than smaller granules. This also makes that the large granules contain relatively more water than small granules. Fig. 2 shows the water content profiles of the large, median and small granules versus time. The water content of the fines (if sufficiently formed) is also depicted. First the characteristic sizes (d_{10}, d_{50} and d_{90}) have been determined as a function of drying time. Subsequently the moisture content of the different size fractions has been determined. The figure shows that the initial water content of the large granules is higher than that of the smaller granules. This water content difference remains throughout the drying process. Large granules consistently contain more water than the small ones. Under all tested conditions (inlet air temperature 40 and 60 °C, inlet air flow 60, 80 or 100 m^3 h^{-1}) the same difference in water content between the granular size fractions is observed.

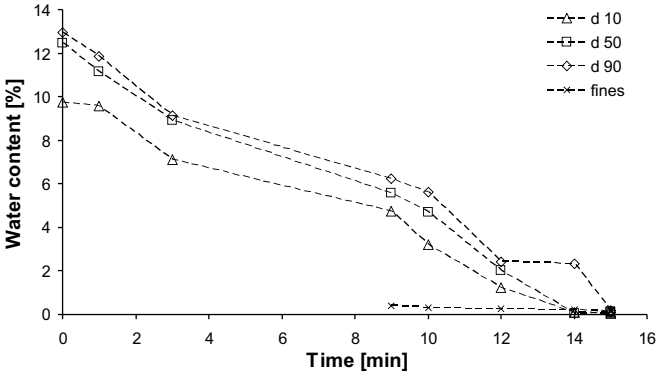

Fig. 2. Water content of the granules versus the drying time. The characteristic sizes (d_{10}, d_{50} and d_{90}) have been determined as a function of time and the moisture contents of the corresponding sieve fractions have been depicted. Temperature incoming air (T_{in}) 40 °C, air velocity 1.8 m s^{-1}. For each time point the water content values of the granules and fines are correlated; the data points per time point all come from one batch.

Fig. 1 shows that the majority of fine particles are formed in the latest stage of drying. Moreover, the small granules show more size reduction earlier in time (Fig. 1) and meanwhile, these granules are dryer than the large ones (Fig. 2). This is an indication that moisture content and fines formation are interrelated. The fines formation rate has been defined. For simplicity reasons it is assumed that the number of impacts is proportional to both the air velocity and the process time. So a granule dried for 4 min at a certain air flow will endure twice the number of impacts compared to a granule dried for 2 min at the same air flow. This occurs of course only above the minimum fluidization velocity of the granule bed. Below this velocity, breakage or formation of fines by impact is assumed to be minimal [25]. In the used equipment the minimal fluidization velocity for wet granules was determined to be 0.6 m s^{-1} (20 m^3 h^{-1}). Upon drying this velocity decreases to 0.3 m s^{-1} (10 m^3 h^{-1}). The air flow has always been significantly higher than the minimum fluidization velocity. So the fines formation has been defined as:

Formation of fines [(w/w) (m^{-3})] = fraction of fines in total mass [w/w]/(impact exposure time [h] × (air flow minus minimal fluidization flow [m^3 h^{-1}])).

This normalization of the data for the number of impacts enables comparison of the different drying regimes (differences in drying time and air flow). In Fig. 3 the formation of fines is plotted versus the bulk water content of the granules. The "bulk" water content is the average water content; no distinction in granule size classes has been made. Below a bulk water content of 6% fines are formed. Fines formation increases dramatically upon further drying while it is nearly absent at higher water levels. When the effects of process conditions (temperature and air flow) are compared, it can be observed from the figure that the formation of fines is mainly dependent on water content. The shape of all curves obtained at different process settings are basically the same. Some effects of process settings, like temperature, may be visible. It is clear, however, that the impact of moisture content on fines formation

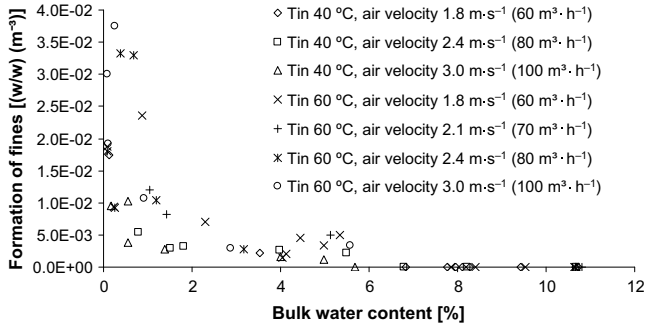

Fig. 3. Formation of fines defined as percentage of total mass divided by the exposure time and divided by the air flow (air flow minus minimal fluidization velocity) versus the bulk water content of the granules. The T_{in} is set at 40 °C or 60 °C.

dominates over all other variables. For each experimental condition, i.e., at varying inlet air temperature and air flow, the same trend is observed.

It has been shown in a previous paper [10] that the change in granule size follows a three phase system characterized by a net growth phase, a plateau phase and a breakage phase. These phases are dependent on the net water content. To distinguish the growth and breakage behavior of the size classes as function of water content more clearly the change in granules size has been plotted versus water content in Fig. 4. The changes in granule size are expressed as

$$\Delta d_x = d_t - d_{t=0} \tag{4}$$

in which d_x can be d_{10}, d_{50} or d_{90}. Hence, Δd_{50} expresses the change in size of the median size granules since the start of the granulation process ($d_{t=0}$). A Δd_{50} above zero reflects a net growth of the granular bulk. In Fig. 4 Δd_x is plotted versus bulk water content. It can be seen that these subsequent phases (i.e., growth, plateau, breakage [10]) are present for all particles, but do not appear at the same bulk water content. As also seen in Fig. 1 at the beginning of the drying process (on the right-hand side of the x-axis) the Δd_{90} values are highly positive, illustrating that the large granules grow initially, which effect is annihilated upon further drying. The d_{50} and d_{10} show hardly any growth. A clear plateau phase, in which granule size does hardly change, is present for d_{50} and d_{90} but not for d_{10}. Clearly, the size classes do show a different behavior during drying. This different behavior is observed under all tested conditions (inlet air temperature 40 and 60 °C, inlet air flow 60, 80 or 100 $m^3\,h^{-1}$). It can be concluded that within a granulate, breakage, growth and the formation of fines are a function of size, composition and water content. Realizing that the strength of granules is determined by water content, which becomes apparent by the different stages (growth, plateau, breakage) in the drying process, it becomes clear why the size fractions do not show these changes simultaneously. Small granules, exhibiting lower water levels early on in the drying process have then already lost their strength and are vulnerable to attrition or breakage. This may account for the fact that also at a relatively high bulk water content (6%) fines are already formed (Fig. 3). Even at the end of the drying process (bulk water content 0.35%) the largest granules still contain a relatively large amount of water. Thus most of the available water is then located in the largest granules. The large granules (d_{90}) consist of small primary particles [2,10] whereas smaller granules consist of larger primary particles. According to Eq. (3) the dynamic strength of the granules increases at decreasing primary particle size. This implies that large granules, composed of small primary particles are stronger [2,10,16]. The total of results should be clarified from this perspective. Theoretically the strength increase is related to the increased total number of contact points between the particles within the granule [2]. As elucidated in the introduction the theory of the dynamic strength only applies for granules that are wetted, i.e saturation is not a part of the equation [2,13]. Also according to Eq.(3), the dynamic strength increases at increasing air velocity as it is assumed that the relative velocity of the moving particles equals the air velocity. Drying at higher air velocity has a number of consequences. The drying process will be faster, but the number of impacts will be higher too. In Fig. 5 the effect of increased air velocity on the granule size is illustrated. Temperature was in this case maintained at 40 °C. As can be seen there a relatively limited growth or breakage effects for the granules exposed to an air velocity of 1.8 m s^{-1} (60 $m^3\,h^{-1}$), whereas granules exposed to the highest air velocity of 3.0 m s^{-1} (100 $m^3\,h^{-1}$) show large effects. Significantly larger size increasing effects or the largest granules and size decreasing effects for the finer granules are seen. Towards the end of the drying process the size increasing effects are annihilated again. At higher air velocity formation of fines starts earlier. The effect of increased air velocity on the water content of granules is illustrated in Fig. 6 for the larger and smaller granules and fines. To further illustrate the effect of granule composition water content is here replaced by the saturation level. According to Eq. (2) composition (reflected in porosity) and water content of a granule determine the sat-

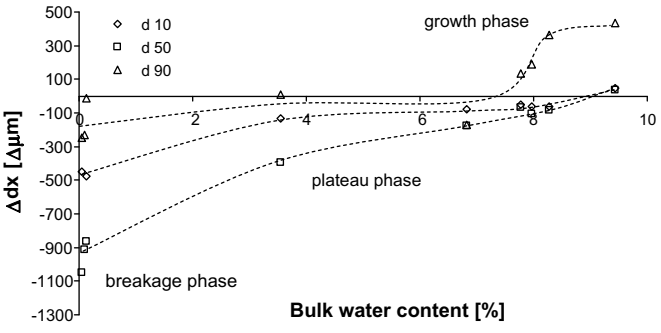

Fig. 4. Growth, plateau and breakage phase as function of bulk water content. T_{in} 40 °C, air velocity 1.8 m s^{-1}.

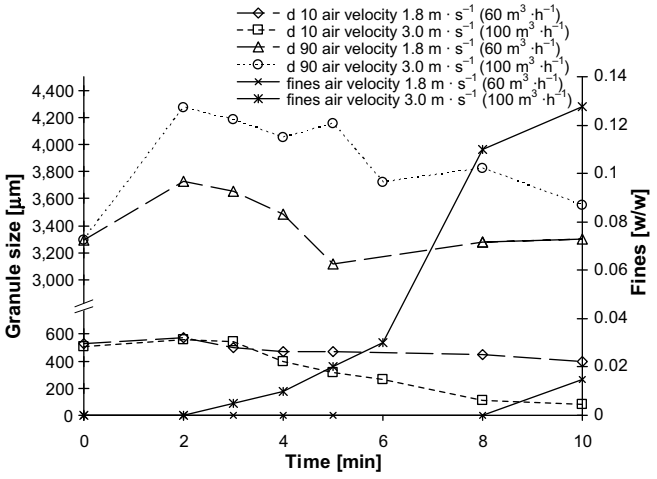

Fig. 5. Granule size versus drying time of granules dried under high or low air velocity. T_{in} 40 °C, air velocity 1.8 m s^{-1} or 3.0 m s^{-1}. On the right-hand axis the formation of fines is shown.

uration level [10]. Smaller granules have intrinsically a lower saturation level than larger granules. Throughout the drying process they will loose water, the binding force, earlier than larger granules. If the primary particle size of the wet granules, the relative velocity of the moving particles, the porosity and viscosity are used to calculate dynamic strength of the granules a strong dependency of primary particle size and composition is seen. A higher air flow and a composition of smaller primary particles lead to a higher dynamic strength of the wet granules. This effect is plotted in Fig. 7. The largest granules (d_{90}) indeed show a velocity dependency which is in-line with theory. The same dependency holds for the small granules (d_{10}), although this is not visible in the resolution of the figure. Smaller granules have under wetted conditions intrinsically a lower dynamic strength. Based upon the saturation level and the dynamic strength small granules will always differentially from large granules throughout the whole drying process.

Process understanding of the fluid-bed drying process implies continuous assessment of process circumstances. Determination of the changes in the humidity of the incoming and outgoing air, the standard process characteristics, do not give direct information on water content of the granules. Direct monitoring of the water content of the lactose granules with NIRS as described in a previous article [16] is used to increase our process understanding of the fluid-bed drying process. It is assumed that the NIR water content determination gives the average water content of the granular bed during the fluid-bed drying process under the tested process conditions [16]. At the start of the drying process it was observed that a change in air velocity above minimal fluidization velocity from 0.6 to 1.8 m s^{-1} resulted in an increase in the NIR water content readings. The increase of the air velocity to the set value is not instantaneous once the process is started. This implies that it takes a significant time (1 min) to develop a completely fluidized bed. As it is shown that smaller granules contain less water

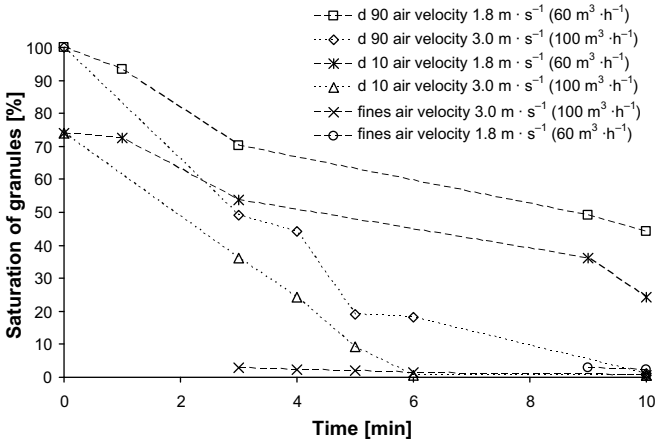

Fig. 6. Saturation level of granules in time. The saturation level of the largest (d_{90}) and smallest granules (d_{10}) are shown in combination with the saturation level of the formed fines. Two air velocities have been used (1.8 and 3.0 m s^{-1}). Values used for calculation ρ_s 1.5, ε 0.15 (d_{10} and fines), 0.165 (d_{90}).

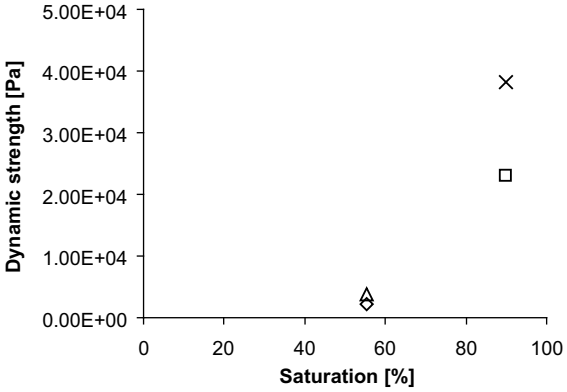

Fig. 7. Dynamic strength versus saturation level of granules after 2 min of drying (T_{in} 40 °C, air velocity 1.8 m s^{-1}). By the water content and composition difference between the granules the saturation level of the small and large granules differs. Values used for calculation ρ_s 1.5, μ 0.001 Pa s Vp 1.8 or 3.0 m s^{-1}, ε 0.15 (d_{10}) and 0.165 (d_{90}), $d_{3,2}$ 4 μm (d_{10}) and 50 μm (d_{90}).

than larger granules, it can be argued that the larger granules are positioned under the smaller granules during the first phase and mix again upon air flow increase. By the NIR method the differences in air flow regime as related to air velocity can be detected; the granular bed size distribution is highly heterogeneous and changes upon air flow increase above minimal fluidization velocity. Besides water content determination the NIR measurements can also be used for granule size analysis [16]. The combination of average water content and average granule size analysis enhances understanding of the fluid-bed drying process.

For high-shear granulated granules containing active material it is known [2] that the behavior of the drug substance is correlated to the particle size. The active drug substance consists in general of very small particles. Preferential growth of the small particles in favor of the larger particles induces in-homogeneity [2]. The current study illustrates that the granular bed, the granule size, the intergranular composition and water content are completely heterogeneous throughout the drying process. This heterogeneity leads to a granule size dependent difference in behavior throughout the fluid-bed drying process.

Attrition, growth, breakage and segregation are unwanted effects of the drying process. The dynamic size-changing effects during the drying process potentially lead to in-homogeneity of drug substance and therefore to lack of content uniformity, which is detrimental for the end product. It has been stated [26] that increasing air flow leads to decreased lumping risk by the reduced contact time of the granules, increased shear stress in the bed and accelerated drying process. In the situation of wet lactose granules we have shown that increase of the air flow rate leads to the formation of larger granules, which seems to be conflicting. However, what is clear from the present study is that water content as well as granule composition should always be a part of the discussion. The increasing shear stress may lead here to increased consolidation and agglomeration tendency upon contact of the granules. Ide-

ally the granular characteristics, with exception of the water content of the granules, do not change at all throughout the process. From the results it can be concluded that the behavior of the large granules differs very much from the behavior of the small granules. When working on quality by design, one should check which consequences this has on the ultimate quality of intermediate and end product.

References

[1] H. Rumpf, Grundlagen und methoden des granulieren, Chemie. Ing. Techn. 30 (1958) 144–158.
[2] K. van den Dries, H. Vromans, Relationship between inhomogeneity phenomena and granule growth mechanisms in a high-shear mixer, Int. J. Pharm. 247 (2002) 167–177.
[3] H. Vromans, H.G.M. Poels-Janssen, H. Egermann, Effects of high shear granulation on granule homogeneity, Pharm. Dev. Technol. 4 (1999) 297–303.
[4] S.M. Iveson, J.D. Litster, K. Hapgood, B.J. Ennis, Nucleation, growth and breakage phenomena in agitated wet granulation processes: a review, Powder Technol. 117 (2001) 3–39.
[5] S.M. Iveson, J.D. Litster, Growth regime map for liquid-bound granules, AIChE J. 44 (1998) 1510–1518.
[6] A. Darelius, H. Brage, A. Rasmuson, I. Niklasson Björn, S. Folestad, A volume based multi dimensional population balance approach for modeling high shear granulation, Chem. Eng. Sci. 61 (2006) 2482–2493.
[7] D.N. Travers Drying, in: M.E. Aulton (Ed.), Pharmaceutics, The Science of Dosage form Design, Churchill Livingstone, Edinburgh, 1988, pp. 629–646.
[8] C.R. Bemrose, J. Bridgewater, A review of attrition and attrition test methods, Powder Technol. 49 (1987) 97–126.
[9] K. van den Dries, O.M. de Vegt, V. Girard, H. Vromans, Granule breakage phenomena in a high shear mixer; influence of process and formulation variables and consequences on granule homogeneity, Powder Technol. 133 (2003) 228–236.
[10] F.J.S. Nieuwmeyer, K. van der Voort Maarschalk, H. Vromans, Granule breakage during drying processes, Int. J. Pharm. 329 (2006) 81–87.
[11] H. Schubert, Tensile strength of agglomerates, Powder Technol. 11 (1975) 107–119.
[12] A. Faure, P. York, R.C. Rowe, Process control and scale-up of pharmaceutical wet granulation processes: a review, Eur. J. Pharm. Biopharm. 52 (2001) 269–277.
[13] B.J. Ennis, J. Li, G.I. Tardos, R. Pfeffer, The influence of viscosity on the strength of an axially strained pendular liquid bridge, Chem. Eng. Sci. 45 (1990) 3071–3088.
[14] T. Schæfer, D. Johnsen, A. Johansen, Effects of powder particle size and binder viscosity on intergranular and intragranular particle size heterogeneity during high shear granulation, Eur. J. Phar. Sci. 21 (2004) 525–531.
[15] A.C. Scott, M.J. Hounslow, T. Instone, Direct evidence of heterogeneity during high shear granulation, Powder Techn. 113 (2000) 205–213.
[16] F. Nieuwmeyer, M. Damen, A. Gerich, F. Rusmini, K. van der Voort Maarschalk, H. Vromans, Granule characterization during fluid-bed drying by development of a near infrared method to determine water content and median granule size, Pharm. Res. 24 (2007) 1854–1861.
[17] S.I. Farag Badawy, M.A. Hussain, Effect of starting material particle size on its agglomeration behavior in high shear wet granulation, AAPS Pharm. Sci. Tech. 5 (2004) 1–7.
[18] Food and Drug Administration, Guidance for industry; PAT—a framework for innovative pharmaceutical development, manufacturing and quality assurance, 2004.
[19] R.L. Green, G. Thurau, N.C. Pixley, A. Mateos, R.A. Reed, J.P. Higgins, In-line monitoring of moisture content in fluid-bed dryers using near-IR spectroscopy with consideration of sampling effects on method accuracy, Anal. Chem. 77 (2005) 4515–4522.
[20] W.P. Findlay, G.R. Peck, K.R. Morris, Determination of fluidized bed granulation end point using near-infrared spectroscopy and phenomenological analysis, J. Pharm. Sci. 94 (2005) 604–612.
[21] P.L.D. Wildfong, A. Samy, J. Corfa, G.E. Peck, K.R. Morris, Accelerated fluid-bed drying using NIR and phenomenological modeling: method assessment and formulation stability, J. Pharm. Sci. 91 (2002) 631–639.
[22] E. Räsänen, J. Rantanen, J. Mannermaa, J. Yliruusi, H. Vuorela, Dehydration studies using a novel multichamber microscale fluid-bed dryer with in-line near-infrared measurement, J. Pharm. Sci. 92 (2003) 2074–2081.
[23] J. Rantanen, S. Lehtola, P. Rämet, J. Mannermaa, J. Yliruusi, On-line monitoring of moisture content in an instrumented fluidized bed granulator with a multichannel NIR moisture sensor, Powder Techn. 99 (1998) 163–170.
[24] D.L. Massart, B.G.M. Vandengiste, L.M.C. Buydens, S. de Jong, P.J. Lewi, J. Smeyers-Verbeke, Handbook of Chemometrics and Qualimetrics: Part A, Elsevier, Amsterdam, 1997, pp. 263–303.
[25] Y. Ray, T. Jiang, Particle attrition phenomena in a fluidized bed, Powder Techn. 49 (1987) 193–206.
[26] S. Palzer, Drying of wet agglomerates in a continuous fluid-bed: influence of residence time, air temperature and air-flow rate on the drying kinetics and the amount of oversize particles, Chem. Eng. Sci. 62 (2007) 463–470.